# Charge-transfer potentials for ionic crystals: Cauchy violation, LO-TO splitting, and the necessity of an ionic reference state

Sergey V. Sukhomlinov* and Martin H. Müser
*Jülich Supercomputer Centre, Institute for Advanced Simulations, FZ Jülich, Jülich, Germany*
(Dated: November 16, 2015)

In this work, we study how including charge transfer into force fields affects the predicted elastic and vibrational Γ-point properties of ionic crystals, in particular those of rock salt. In both analytical and numerical calculations, we find that charge transfer generally leads to a negative contribution to the Cauchy pressure, $P_{\rm C} \equiv C_{12} - C_{66}$, where $C_{12}$ and $C_{66}$ are elements of the elastic tensor. This contribution increases in magnitude with pressure for different charge-transfer approaches in agreement with results obtained with density functional theory (DFT). However, details of the charge-transfer models determine the pressure dependence of the LO-TO splitting and that for partial charges. These last two quantities increase with density as long as the chemical hardness depends at most weakly on the environment while experiments and DFT find a decrease. In order to reflect the correct trends, the charge-transfer expansion has to be made around ions and the chemical (bond) hardness has to increase roughly exponentially with inverse density or bond lengths. Lastly, the adjustable force-field parameters only turn out meaningful, when the expansion is made around ions.

PACS numbers: 34.20.-b, 34.20.Cf, 62.20.D-. 34.70.+e

## I. INTRODUCTION

A prominent manifestation of many-body interactions is the violation of Cauchy relations in situations where they would hold if atoms interacted in a pair-wise fashion: crystals near mechanical equilibrium, in which all atoms occupy centrosymmetric positions [1]. Cauchy violations are quantified in terms of so-called Cauchy pressures, e.g., $P_{\rm C} \equiv C_{12} - C_{66}$, the only Cauchy pressure for crystals of cubic symmetry. Reproducing large *positive* Cauchy pressures typical for simple metals received significant attention in the context of embedded-atom and related models [2–4]. In contrast to metals, many alkali halogens, in particular those composed by light elements, have a *negative* $P_{\rm C}$, whose magnitude can even exceed $0.2\ C_{12}$ [5]. Another manifestation of many-body effects is that infrared spectra can in general not be described accurately in terms of models assuming constant atomic charges or constant dipoles [6].

Different approaches have been pursued to describe many-body effects in simple ionic solids. Early many-body potentials for ionic compounds assumed polarizable anions and placed shells [7] or classical Drude oscillators [8, 9] on them. By now it has become good practice to include dipolar and even quadrupolar polarizability into force fields, e.g., for the simulation of ionic liquids [10]. However, inducible dipoles, or other multipoles below hexadecupoles, cannot account for a non-zero Cauchy pressure (in rocksalt), because they remain zero upon a homogeneous deformation of a centro-symmetric crystal so that only two-body interactions account for its elastic tensor. More recent approaches assume that ions can change their size [11] and later also their shape [12] in response to their environment, whereby they effectively introduce short-range many-body interactions. Properly parametrized models of these so-called breathing-shell potentials [13, 14] can then correctly describe the elasticity of ionic solids.

Despite the success of breathing-shell models, the assumption of a constant partial charge may not always be justified. Even in a homogeneous system like rock salt one may expect that a certain amount of charge is redistributed between atoms when a crystal is deformed. In fact, the quantum mechanical ground state of a hypothetical NaCl crystal with infinitely large lattice constant is composed of neutral atoms rather than of ions [15]. As a consequence of charge redistribution, the force on an atom induced by a (local) electrostatic field can be affected by the deformation of the crystal. This, however, is not properly reflected in fixed-charge models. Charge-transfer potentials (CTP) [16–20] — in particular those based on the electronegativity principle proposed by Sanderson [21] — can overcome this limitation.

In this work, we study analytically and by means of computer simulations how including charge transfer into force fields affects the elastic and vibrational (Γ-point) properties of (centrosymmetric) ionic solids. Towards this end, we focus on NaCl in the rocksalt structure, for which we develop an interaction model that only contains two-body short-range repulsion and charge-transfer related energies. Regarding elasticity, our emphasis lies on the Cauchy pressure and how it changes with density. As finite Cauchy pressures are solely due to charge transfer between atoms in CTP-based force field that contain no additional many-body interactions, we also study how partial charges change with density. Since the splitting of longitudinal optical (LO) and transverse optical (TO) is in turn related to Born effective charges, we also investigate the pressure-dependence of the LO-TO frequency

* s.sukhomlinov@fz-juelich.de

splitting in the center of the Brillouin zone.

A highly accurate and transferable potential certainly necessitates many-body contributions in addition to charge transfer terms, for example, those contained in breathing shell or quantum Drude oscillator models. They would affect the predictions for elasticity and LO-TO splitting. However, we ignore these contributions, because our objective is to scrutinize the generic properties of charge-transfer potentials rather than to develop a highly-accurate interaction potential for rock salt.

The remainder of this work is structured as follows: Section II contains numerical methods and some theoretical background, specifically a brief review on classical elasticity theory for finite stress, a generalization of the Cauchy violation to non-zero pressure, and the definition of Born effective charge (tensors) or Bader charge. Additionally, we present the DFT methodology that was used to produce the reference data for NaCl. The general form of CTPs are described in Section III, where we also derive how CTPs affect the Cauchy pressure and partial charges, which in turn drive the LO-TO splitting. In section IV, we parametrize different CTP approaches and compare the predictions of the respective force-field based simulations to analytical formulae and DFT results. Conclusions are drawn in section V.

## II. METHODS AND THEORETICAL BACKGROUND

### A. Elasticity at zero and non-zero stress

In this section, we review basic aspects of the theory of elasticity at finite stress. We see such an overview as necessary because we are not aware of a compact representation that explains why the definition of elastic strain is not unique and how seemingly subtle differences between them — as well as the choice of the thermodynamic reference potential — affects the results for elastic constants. The presented subtleties are irrelevant for most solids at ambient pressures, but care needs to be taken whenever the bulk or the shear modulus of a solid is no longer large compared to an external stress. Therefore, we repeat common definitions for strain, stress, and elastic tensors, which become relevant at large pressure $P$, and summarize their mutual relations. This includes a generalization of the Cauchy violation to finite pressures.

We note that the full tensor notation is used only here in section II A, while Voigt notation is employed outside of it. In the Voigt notation, pairs of indices are lumped into a single index. For example, selected strain tensor components read $\varepsilon_{11} \to \varepsilon_1$ and $\varepsilon_{12} \to 2\varepsilon_6$.

#### 1. *Strain tensors*

Solids deform under a *change* of external stress. Mathematically, the deformation is stated by a mapping $\mathbf{x}(\mathbf{X})$, where $\mathbf{X}$ denotes a (Cartesian) coordinate of one particular material point in the original reference structure and $\mathbf{x}$ denotes the final position of the same material point.

In this work, we restrict our attention to linear mappings for which the displacement field

$$\mathbf{u}(\mathbf{X}) \equiv \mathbf{x}(\mathbf{X}) - \mathbf{X} \tag{1}$$

is a linear function of $\mathbf{X}$. Component by component, Eq. (1) reads $u_\alpha = x_\alpha - X_\alpha$ with $\alpha = 1, 2, 3$. To describe (the rotationally invariant part of) linear deformations, two (symmetric) tensors of rank two can be defined.

The **Eulerian strain tensor** [22] is defined by

$$\varepsilon_{\alpha\beta} = \frac{1}{2}\left(\frac{\partial u_\alpha}{\partial X_\beta} + \frac{\partial u_\beta}{\partial X_\alpha}\right). \tag{2}$$

It relates the original coordinate — up to a rotation — to the final coordinate via the linear transformation

$$x_\alpha = (\delta_{\alpha\beta} + \varepsilon_{\alpha\beta})X_\beta, \tag{3}$$

where we have used, as we will in the following, the Einstein summation convention. Since $\varepsilon$ is symmetric, it has six independent coefficients in three-dimensional space.

The **Lagrangian strain tensor** $\eta$ [23] — also known as Green-Lagrangian finite-strain tensor — is defined such that the squared vector length of any final coordinate in a linear mapping is given by

$$\mathbf{x}^2 = \mathbf{X}^2 + 2\eta_{\alpha\beta}X_\alpha X_\beta. \tag{4}$$

The components of the Lagrangian strain tensor are given by

$$\eta_{\alpha\beta} = \frac{1}{2}\left(\frac{\partial u_\alpha}{\partial X_\beta} + \frac{\partial u_\beta}{\partial X_\alpha} + \frac{\partial u_\gamma}{\partial X_\alpha}\frac{\partial u_\gamma}{\partial X_\beta}\right). \tag{5}$$

The two strain tensors are only equivalent up to linear order. Their relation can be expressed as:

$$\eta_{\alpha\beta} = \varepsilon_{\alpha\beta} + \frac{1}{2}\varepsilon_{\alpha\gamma}\varepsilon_{\gamma\beta} \tag{6}$$

$$\varepsilon_{\alpha\beta} = \eta_{\alpha\beta} - \frac{1}{2}\eta_{\alpha\gamma}\eta_{\gamma\beta} + O(\eta^3). \tag{7}$$

Since Eulerian and Lagrangian strain tensors are equivalent only in the first order, the second derivatives or the second-order expansion coefficients of a quantity $T$ (taken with respect to the strain tensor components) are not identical unless the first derivatives disappear. This can be seen from expressing the Taylor series expansion of a function $T$

$$T = T_0 + T^{(\eta)}_{\alpha\beta}\eta_{\alpha\beta} + \frac{1}{2}T^{(\eta)}_{\alpha\beta\gamma\delta}\eta_{\alpha\beta}\eta_{\gamma\delta} + O(\eta^3) \tag{8}$$

in terms of $\varepsilon$. Substituting equation (6) into (8) and

rearranging terms yields

$$T = T_0 + T^{(\eta)}_{\alpha\beta}\varepsilon_{\alpha\beta} + \frac{1}{2}\left(T^{(\eta)}_{\alpha\beta\gamma\delta} + T^{(\eta)}_{\alpha\delta}\delta_{\beta\gamma}\right)\varepsilon_{\alpha\beta}\varepsilon_{\gamma\delta} + \ldots, \tag{9}$$

where $\delta_{\beta\gamma}$ is the Kronecker delta. Thus, by comparing coefficients, one can conclude that the first derivatives with respect to $\eta$ or $\varepsilon$ coefficients are identical and that the second-order coefficients obey

$$T^{(\varepsilon)}_{\alpha\beta\gamma\delta} = T^{(\eta)}_{\alpha\beta\gamma\delta} + T^{(\eta)}_{\alpha\delta}\delta_{\beta\gamma} \tag{10}$$

In this expansion, we have not yet exploited the symmetry of the strain tensor. Since $\varepsilon_{\alpha\beta} = \varepsilon_{\beta\alpha}$, any tensor can be symmetrized accordingly. For example, when using

$$T^{\mathrm{sym}}_{\alpha\beta\gamma\delta} = \frac{1}{4}\left(T_{\alpha\beta\gamma\delta} + T_{\alpha\beta\delta\gamma} + T_{\beta\alpha\gamma\delta} + T_{\beta\alpha\delta\gamma}\right) \tag{11}$$

in a Taylor series expansion instead of the original second derivatives, the result remains unchanged. In the following, we assume that all tensors are symmetrized. Second-order expansion coefficients then obey

$$\Delta T_{\alpha\beta\gamma\delta} = \frac{T^{(\eta)}_{\alpha\delta}\delta_{\beta\gamma} + T^{(\eta)}_{\alpha\gamma}\delta_{\beta\delta} + T^{(\eta)}_{\beta\delta}\delta_{\alpha\gamma} + T^{(\eta)}_{\beta\gamma}\delta_{\alpha\delta}}{4}, \tag{12}$$

where $\Delta T \equiv T^{(\varepsilon)} - T^{(\eta)}$. Selected components are

$$\Delta T_{1111} = T_{11} \tag{13}$$

$$\Delta T_{1122} = 0 \tag{14}$$

$$\Delta T_{1212} = \frac{1}{4}\left(T_{11} + T_{22}\right), \tag{15}$$

which are useful relations for the analysis of elastic tensors for (cubic) systems under finite stress.

As an example, we consider the volume. If $V_0$ denotes the volume of the reference structure, the volume of a strained structure is

$$V = V_0 \begin{vmatrix} 1+\varepsilon_{11} & \varepsilon_{12} & \varepsilon_{13} \\ \varepsilon_{12} & 1+\varepsilon_{22} & \varepsilon_{23} \\ \varepsilon_{13} & \varepsilon_{23} & 1+\varepsilon_{33} \end{vmatrix}. \tag{16}$$

Thus, the relative volume change, $\Delta v \equiv (V - V_0)/V_0$ to second order in $\varepsilon$ is

$$\begin{aligned}\Delta v = {} & \varepsilon_{11} + \varepsilon_{22} + \varepsilon_{33} + \varepsilon_{11}\varepsilon_{22} + \varepsilon_{22}\varepsilon_{33} + \varepsilon_{33}\varepsilon_{11} \\ & - \left(\varepsilon^2_{12} + \varepsilon^2_{13} + \varepsilon^2_{23}\right).\end{aligned} \tag{17}$$

Substitution of eq. (7) into the above equation gives

$$\begin{aligned}\Delta v = {} & \eta_{11} + \eta_{22} + \eta_{33} + \eta_{11}\eta_{22} + \eta_{22}\eta_{33} + \eta_{33}\eta_{11} \\ & - \frac{1}{2}\left(\eta^2_{11} + \eta^2_{22} + \eta^2_{33}\right) - 2\left(\eta^2_{12} + \eta^2_{13} + \eta^2_{23}\right).\end{aligned} \tag{18}$$

One can see that $\partial^2\Delta v/\partial\varepsilon^2_{12} = -2$, while $\partial^2\Delta v/\partial\eta^2_{12} = -4$. The difference between these second derivatives is equal to $\partial\Delta v/\partial\eta_{11} + \partial\Delta v/\partial\eta_{22}$. When considering the degeneracy factor of the expansion, this result is readily seen to be consistent with equation (15).

In reference to computer simulation of periodically repeated cells, we note that the Eulerian strain is useful when taking numerical derivatives of the energy with respect to strain and even more so in the context of constant stress simulations, in which case the six independent tensor components are treated as dynamical variables. If the vectors spanning the simulation box are arranged in a matrix $h$, the component of a real coordinate (of unit length) is given by $R_\alpha = h_{\alpha\beta}\tilde{R}_\beta$, where $\tilde{\mathbf{R}}$ with $0 \leq \tilde{R}_\alpha < 1$ denotes a reduced cell coordinate. Deformation of the reference box can then be described in a straightforward fashion by

$$h_{\alpha\beta} = (\delta_{\alpha\gamma} + \varepsilon_{\alpha\gamma})h^{\mathrm{ref}}_{\gamma\beta}, \tag{19}$$

where $h^{\mathrm{ref}}$ is the reference h-matrix, e.g., the expected average shape of the simulation cell at the reference pressure.

### *2. Stress and elastic tensors*

Stress and elastic or stiffness tensors can be loosely defined as the first and the second derivative of the energy density of a solid with respect to the strain. These lax definitions are sufficient for practical purposes when both external stress and thermal fluctuations can be considered small. Numerical values for the pertinent tensor elements are then automatically close to those deduced from acoustic phonons or stress-strain measurements [24]. Once stress can no longer be conidered small, the elastic tensor elements differ between the two strain defintions. Once thermal fluctuations start to matter (as well), different results can be obtained depending on which thermodynamic potential $T$ is converted into energy density. Candidates are internal energy $U$, free energy $F$, enthalpy $H$, Gibbs free energy $G$, or for non-isotropic stresses, an appropriate generalization of the Gibbs free energy. Since we do not examine finite temperature in this work, we consider the thermodynamic potentials $U$ and $H$ (both evaluated at zero temperature) by default. Readers interested in finite temperature elasticity and Maxwell relations for elastic tensors may consider reading Ref. 25.

In the last section, we showed that the first derivative of an arbitrary function with respect to strain does not depend on which definition for strain is used. Thus, we obtain the same stress tensor $\sigma$ when defining it as the first derivative of the energy with respect to either Eulerian or Lagrangian strain. Such an equivalence no longer holds for the second derivatives.

Different names are used for the elastic constants in the literature depending on the choice of thermodynamic potential and strain [24, 26, 27]. For example, Voigt (Brugger) constants are the second derivative of the internal energy density with respect to Eulerian (Lagrangian)

strain [27]. In addition, at non-zero temperature, one can distinguish between isothermal and adiabatic elastic constants, depending on the thermodynamic boundary conditions or the choice of the thermodynamic potential [28].

To avoid confusion between the zoo of possible definitions for elastic tensor elements, we specify elastic constants with two superscripts. The first gives the thermodynamic potential and the second provides the strain definition, for example,

$$C^{H\eta}_{\alpha\beta\gamma\delta} \equiv \frac{1}{V_0}\frac{\partial^2 H}{\partial\eta_{\alpha\beta}\partial\eta_{\gamma\delta}}. \tag{20}$$

These coefficients are called the Birch coefficients [26]. The tensor of Birch coefficients has special significance, because it has to be positive definite in order for a structure to be stable at constant pressure [29, 30].

In numerical calculations of stiffness coefficients, it is easiest to work with the Eulerian strain and the internal energy. To determine elements of $C^{U\varepsilon}_{\alpha\beta\gamma\delta}$ of a cubic structure, it is then beneficial to know the relation between the bulk modulus

$$B \equiv -\frac{\partial P}{\partial \ln V} \tag{21}$$

and the $C^{U\varepsilon}_{\alpha\beta\gamma\delta}$. For an isotropic pressure, applied to a solid of cubic symmetry, it is readily shown that

$$C^{U\varepsilon}_{1122} = \frac{3}{2}B - \frac{1}{2}C^{U\varepsilon}_{1111} - \frac{P}{2}. \tag{22}$$

By applying equation (10) to equation (22), the Lagrange-strain-based elastic tensor can be calculated in a straightforward fashion from the Euler-strain-based one, where $T_{\alpha\beta}$ corresponds to the stress tensor element $\sigma_{\alpha\beta}$. As a result, one obtains

$$C^{U\eta}_{1111} = C^{U\varepsilon}_{1111} + P \tag{23}$$
$$C^{U\eta}_{1122} = C^{U\varepsilon}_{1122} \tag{24}$$
$$C^{U\eta}_{1212} = C^{U\varepsilon}_{1212} + P/2. \tag{25}$$

#### 3. *Cauchy relations for central potentials at finite stress*

The Cauchy relations state that the elastic tensor of a crystalline structure is symmetric in all indices, e.g., $C_{1212} = C_{1122}$ [1]. They hold, for non-fortuitous reasons, if atoms sitting on symmetry sites interact through central potentials and thermal (or ionic quantum) fluctuations are negligible. At finite pressures, Cauchy relations are valid only for $C^{U\eta}_{\alpha\beta\gamma\delta}$, as we quickly demonstrate in the following.

Let us denote atomic coordinates in the reference frame by $\mathbf{R}_i$ and in the strained lattice by $\mathbf{r}_i$. For central potentials, the total energy of a (strained) crystal can be written as

$$U = \sum_{i,j>i} W_{ij}(r^2_{ij}), \tag{26}$$

where $r^2_{ij}$ is the squared distance between atoms $i$ and $j$ and $W_{ij}$ a distance-dependent two-body potential. The energy can be differentiated twice with respect to Lagrangian strain tensor components using equation (4). The result of the differentiation gives the elastic tensor elements at the reference structure

$$C^{U\eta}_{\alpha\beta\gamma\delta} = 4\sum_{i,j>i} R_{ij,\alpha}R_{ij,\beta}R_{ij,\gamma}R_{ij,\delta}W''_{ij}(R^2_{ij}), \tag{27}$$

if not only the initial but also the final atomic positions $\mathbf{r}_i$ correspond to equilibrium (symmetry) sites. Obviously, the $C^{U\eta}$ stiffness tensor remains invariant to any permutation of indices. Thus, the $C^{U\eta}$ satisfy the Cauchy relation not only at zero but any isotropic stress under the given conditions. We therefore define a general expression for Cauchy pressure as

$$P_{\mathrm{c}} = C^{U\eta}_{12} - C^{U\eta}_{44} \tag{28}$$

### B. Bader and Born effective charges

A central aspect of this work is to investigate how charge-transfer potentials affect the violation of the Cauchy relations, whereby we correlate a (predicted) deformation-induced redistribution of charge and the Cauchy pressure. It is certainly desirable to also directly compare the predicted charge redistribution to those of full quantum-mechanical treatments. Doing this is difficult, because charge distribution in our force-field description is fully characterized by partial atomic charges, which, however, are not uniquely defined in a full quantum-mechanical treatment [31–35].

Despite these difficulties, there are well-defined quantities that reflect charge (re)distribution in both force-field-based and full electronic-structure approaches. One such quantity is the Born effective charge (tensor), which has, amongst others, the following advantages: first, unlike some other charge-assignment schemes, its definition does not require biased input. Second, the Born effective charge (tensor) follows from the redistribution of electron density that occurs in response to a (non-homogeneous) deformation, i.e., it relates to a change of charge distribution rather than to "absolute charges". Third, the Born effective charge can be deduced experimentally from the LO-TO splitting given that the high-frequency dielectric permittivity is known [36, 37].

The elements of the Born effective charge tensor of a given atom $i$ (in a finite system, i.e., one in which no periodic boundary conditions apply) can be defined as

$$Q^*_{i,\alpha\beta} \equiv \frac{\partial \mu_\alpha}{\partial r_{i,\beta}}, \tag{29}$$

where $\mu_\alpha$ is the $\alpha$ component of the total dipole of the system.

Unfortunately, dipoles cannot be uniquely defined in periodically repeated system. However, one can relate the dipole to the polarization $\mathbf{p}$ times the primitive cell volume $\Omega$ and consider the pertinent expression in Fourier space in the long wavelength limit [38]. This leads to an alternative definition of the Born effective charge tensor in periodically repeated systems as

$$Q^*_{i,\alpha\beta} \equiv \Omega \lim_{|\mathbf{k}|\to 0} \frac{\partial \tilde{p}_\alpha(\mathbf{k})}{\partial \tilde{r}_{i,\beta}(\mathbf{k})}\bigg|_{\boldsymbol{E}=0}, \tag{30}$$

while setting macroscopic electric field $\mathbf{E}$ to zero. We note that the charge tensor of an atom located in a cubic environment has only one independent component $Q^*_i$, i.e., $Q^*_{i,\alpha\beta} = Q^*_i \delta_{\alpha\beta}$. In this case one can call it the Born effective charge.

A disadvantage of the Born effective charge for the present purpose is that it contains distributions related to the polarization within an atom, i.e., the Born effective charge of a fixed-charge, inducible-dipole potential is not constant. Since we ignore such polarizability, we may not be in a position to reproduce the Born effective charge to a high accuracy, the more so as it can (and does, see the result section) exceed an elementary charge in alkali halides. We therefore also consider Bader charges [32] as an alternative, unambiguous charge assignment scheme. Bader divides the space into regions separated by the zero-flux surface of the electron density. Each such region contains a nucleus and all electron density in that region is assigned to that nucleus. In this work, we used the Bader Charge Analysis code as described in references 39–41.

### C. DFT methods

In order to have full control over the proper definition of elastic tensor elements we decided to parametrize and compare our force-field approach only to density-functional theory (DFT) [42, 43] results rather than to experiments. However, we chose the DFT method which best reproduced experimental results. In addition, by comparing to DFT simulations, we can deduce Born effective charges at any given stress or density.

All calculations were performed using DFT as implemented in the QUANTUM ESPRESSO code [44]. To identify a suitable DFT method for our purpose, we investigated different combinations of exchange-correlation functionals and basis sets. Among the available functionals we chose the approximations for exchange-correlation functionals by Perdew, Burke and Ernzerhof [45] (PBE), Becke, Lee, Yang and Parr (BLYP) [46] as well as Perdew and Wang [47] (PW91). As pseudopotentials we considered norm-conserving Trouiller-Martins (MT) [48], norm-conserving Hartwigsen-Goedecker-Hutter-Teter [49] and the projector augmented wave (PAW) basis [50]. All pseudopotentials were downloaded from the QUANTUM ESPRESSO library. We ensured convergence with respect to the plane-wave cutoff energy together with the Monkhorst-Pack sampling of the Brillouin zone [51] in all runs.

Out of the tested combinations, we found that PBE+PAW (PBE functional combined with projected-augmented waves basis) and PW91+MT (PW91 functional combined with Trouiller-Martins norm-conserving pseudopotential) reproduced best the ratios of the different elastic tensor elements that were measured experimentally at low temperature. Out of these two, we chose PW91+MT, as it was closer to low-temperature experimental results (see Table I). For this combination, it proofed sufficient to truncate the plane-wave expansion of the electronic wavefunctions at 110 Ry and to sample the Brillouin zone on a 14x14x14 Monkhorst-Pack mesh.

## III. CHARGE-TRANSFER POTENTIALS

Polarizable force fields approximately describe the redistribution of charge induced by deformations of molecules and solids. Phenomenologically, one can distinguish between on-site polarizability, e.g., in the form of inducible point dipoles [56], and/or, charge transfer between sites [19]. In this work, we only consider the latter for mainly two reasons. First, in simple ionic compounds, crystalline positions lie on symmetry sites so that no dipoles develop during a homogeneous deformation. Second, including on-site polarizability complicates all analytical expressions without affecting qualitatively results deduced in this work.

### A. General formulation

In the present work we consider a force field of the form

$$U = U_{\mathrm{SR}} + U_{\mathrm{CTP}} \tag{31}$$

where $U_{\mathrm{SR}}$ is a two-body, short-range potential and $U_{\mathrm{CTP}}$ a charge-transfer potential.

The simplest and most successful functional form for short-range repulsion is a simple exponential [57],

$$U_{\mathrm{SR}} = \sum_{i,j<i} U_{0,ij}\, e^{-r_{ij}/a_{ij}}, \tag{32}$$

where $U_{0,ij}$ and $a_{ij}$ are parameters of unit energy and length, respectively. For NaCl in the rocksalt structure, one usually only considers short-range repulsion between (adjacent) sodium and chlorine ions, although we also include short-range repulsion between chlorine ions.

The charge-transfer potential allows one to assign partial atomic charges on the fly. In general, the assignment of charges is done following a minimization principle. Here, we consider the split-charge equilibration

| | $a_0$ | $B_0$ | $-P_C$ | $P_A$ | $\omega_{LO}$ | $\omega_{TO}$ | $P(V_{1,2})$ | $\chi^2_{PW91+MT}$ | $\chi^2_{exp}$ |
|---|---|---|---|---|---|---|---|---|---|
| PW91+MT | 5.628 | 23.9 | 1.55 | -4.43 | 245.9 | 149.5 | 6.77, -3.18 | n.a. | 1.59 |
| PBE+PAW | 5.689 | 23.2 | 0.54 | -5.30 | 243.3 | 150.3 | 8.43, -2.75 | 0.94 | 1.71 |
| exp [52] | 5.634 | 28.0 | | | | | 8.93, -3.29 | 2.22 | n.a. |
| exp [53] | 5.640 | 23.8 | | | 257.0 | 164.7 | | | |
| exp [54] | | 26.6 | 2.08 | -9.74 | | | | | |
| exp [55] | | 27.4 | 1.39 | -9.90 | | | | | |

TABLE I. Data contained in the learning set (PW91+MT). For comparison, we include an alternative DFT method (PBE+PAW) as well as experimental values. When comparing to experimental data, we always choose the most recent experiment (i.e., the top one). $P_A$ is the "anisotropy pressure", which we define as $C_{44} - (C_{11} - C_{12})/2$. The units are Å for length, GPa for pressure, and $cm^{-1}$ for frequencies.

(SQE) model [19] as a prototypical charge transfer potential. It is a hybrid between the traditional electronegativity equalization model (EEM) [16] and the atom-atom charge transfer (AACT) model [18]. Recently, SQE has been derived from a controlled approximation of density functional theory [20].

In SQE, an atomic charge is written as

$$Q_i = \sum_j q_{ij}, \tag{33}$$

where $q_{ij}$ represents the amount of charge transferred from atom $j$ to atom $i$, which implies the antisymmetry of $q$: $q_{ij} = -q_{ji}$. The total charge-transfer potential to be minimized in SQE reads:

$$U^{tot}_{CTP} = \sum_i \left(\chi_i Q_i + \frac{1}{2}\kappa_i Q_i^2\right) + \frac{1}{2}\sum_i \sum_{j>i} \kappa_{ij} q_{ij}^2 + \frac{1}{2}\sum_i \sum_{j\neq i} J_{ij}(r_{ij}) Q_i Q j. \tag{34}$$

The first-order parameter $\chi_i$ and the second-order parameter $\kappa_i$ are the atomic electronegativity and hardness respectively [17], $\kappa_{ij}$ is called the hardness of the bond connecting atoms $i$ and $j$ (similar to the one introduced in Ref. 58). EEM is obtained in the limit $\kappa_{ij} \to 0$, while AACT corresponds to $\kappa_i \to 0$. $J_{ij}(r_{ij})$ represents the electrostatic interaction between two atoms. Various terms appearing in equation (34) are now discussed in more detail.

In our parameterization, we use the Mulliken definition of atomic electronegativity and hardness, which both represent the finite difference approximation of the electron energy with respect to the total number of electrons,

$$\chi_i = \frac{I_i + A_i}{2} \tag{35}$$

$$\kappa_i = I_i - A_i. \tag{36}$$

Here, $I_i$ and $A_i$ are atomic ionization energies and electron affinities, respectively.

The electrostatic potential $J_{ij}(r_{ij})$ in equation (34) is often approximated as a Coulomb interaction between point charges. Sometimes, however, the singularity of the Coulomb interaction is screened, e.g., via

$$J_{ij}(r_{ij}) = \frac{\mathrm{erf}(\alpha_{ij} r_{ij})}{r_{ij}}. \tag{37}$$

It represent the coupling between two Gaussian charge distributions $g(\mathbf{r})$ given by

$$g_i(\mathbf{r}) = \left\{\frac{1}{2\pi\rho_i^2}\right\}^{3/2} \exp(-(\mathbf{r} - \mathbf{r}_i)^2/2\rho_i^2), \tag{38}$$

where $\mathbf{r}_i$ is the position of atom $i$, while $\rho_i$ can be viewed as an effective radius of atom $i$. For this Gaussian charge distribution, the parameter $\alpha_{ij}$ in (37) reads

$$\alpha_{ij} = \left(\frac{1}{2\rho_i^2 + 2\rho_j^2}\right)^{1/2}. \tag{39}$$

### 1. *Application to the rocksalt structure*

When considering neutral atoms as reference, the energy per atom in the rocksalt structure can be written in a compact form as

$$U_{CTP} = \Delta\chi Q + \frac{1}{2}\kappa_C Q^2. \tag{40}$$

Here, $Q$ represents the charge on a sodium atom and $\Delta\chi$ is the electronegativity difference normalized to atoms rather than to dimers, that is,

$$\Delta\chi \equiv (\chi_{Na} - \chi_{Cl})/2. \tag{41}$$

The term $\kappa_C$ includes all hardnesses summarized in

$$\kappa_T = \frac{\kappa_{Na} + \kappa_{Cl}}{2} + \frac{\kappa_{NaCl}}{12} \tag{42}$$

as well as the Coulomb interaction, i.e.,

$$\kappa_{\mathrm{C}} = \kappa_{\mathrm{T}} - \frac{\alpha_{\mathrm{M}}(\eta)}{a}, \tag{43}$$

where $\alpha_{\mathrm{M}}(\eta)$ represents the Madelung "constant", which we consider a function of the strain. In the case of screened Coulomb potentials, it also depends on the reference bond length $a$.

The charge minimizing $U_{\mathrm{CTP}}$ is

$$Q = -\Delta\chi/\kappa_{\mathrm{C}} \tag{44}$$

so that the minimized energy reads

$$U_{\mathrm{CTP}} = -\Delta\chi^2/2\kappa_{\mathrm{C}}. \tag{45}$$

### B. Redox-reactive charge-transfer potentials

Chemical reactions, in particular redox reactions, usually imply a quasi-discontinuous change of the electronic structure upon small atomic displacements. Such sudden changes are not captured by force fields assigning a unique potential energy surface that smoothly evolves as a function of atomic coordinates. The description of (redox) reactions requires one to formulate potentials on different energy surfaces, that is, one needs a description not only for the quantum mechanical ground state surface (whose energy generally does evolve smoothly with coordinates) but also for excited states.

In the context of modeling redox reactions with CTPs, it was recently proposed to include a formal oxidation number $n_i$ for each atom as a discrete variable such that the set of oxidation number defines the Landau Zener level on which the system is moving [15, 59]. An atomic charge — in the redox split-charge equilibration (R-SQE) method — then reads

$$Q_i = n_i e + \sum_j q_{ij}. \tag{46}$$

We refer to the literature for technical details [59, 60] and also discuss some aspects in section III B 1. Here, it shall suffice to state that the inclusion of formal oxidation numbers (a) allows one to extend simulations to non-equilibrium situations, such as they occur, for example during triboelectrification [59], or the discharge of a Galvanic element [60, 61], (b) is needed to properly describe the polarizability of zwitter-ionic molecules [62], (c) does not require one to make major modifications to the formulae derived in this manuscript for conventional CTPs, however, (d) does require one, in principle, to assign (independent) interaction parameters for each oxidation state of an element.

#### 1. Application to the rocksalt structure

Expressing the CTP energy in the R-SQE formalism can be done in a similar fashion as in CTPs having neutral atoms as reference. This time, the energy reads

$$U_{\mathrm{R-SQE}} = \Delta\chi_{\mathrm{R}}(Q-1) + \frac{\kappa_{\mathrm{R}}}{2}(Q-1)^2 - \frac{\alpha_{\mathrm{M}}}{2a}Q^2, \tag{47}$$

where $\Delta\chi_{\mathrm{R}}$ is now defined with respect to the ionized states, i.e., $\Delta\chi_{\mathrm{R}} = (\chi_{\mathrm{Na^+}} - \chi_{\mathrm{Cl^-}})/2$, $\kappa_{\mathrm{R}}$ is the (total) chemical hardness relevant for the ionized or redox reference state without Coulomb interactions, i.e., the analogue to $\kappa_{\mathrm{T}}$ introduced in the previous section.

By regrouping the terms in equation (47), $U_{\mathrm{R-SQE}}$ can be brought into the same functional form as the conventional CTP energy in equation (40):

$$U_{\mathrm{R-SQE}} = \mathrm{const} + (\Delta\chi_{\mathrm{R}} - \kappa_{\mathrm{R}})Q + \left(\kappa_{\mathrm{R}} - \frac{\alpha_{\mathrm{M}}}{a}\right)\frac{Q^2}{2}, \tag{48}$$

where $\mathrm{const} = \kappa_{\mathrm{R}}/2 - \Delta\chi_{\mathrm{R}}$.

Equation (48) reveals that — at this level of theory — there are no formal differences between a CTP expansion around neutral atoms or ions, at least as long as we disregard an environment dependence of the hardness terms. Thus, a potential based on R-SQE can be parametrized to give identical results to those of a CTP with neutral atoms in the reference. The only difference lies in the numerical values of the coefficients and their interpretation.

### C. Environment-dependent redox charge-transfer potentials

So far, we have treated all potential interaction parameters as being constant. The underlying assumption is that quantities such as atomic hardness or electronegativity are (effectively) only mildly environment dependent. However, there is at least one parameter in our model for which this assumption may be poorly justified. According to Cioslowski [58], the chemical bond hardness has exponential asymptotics at large atomic separation. Its specific distance or environment dependence for bond lengths close to equilibrium may no longer satisfy the exponential asymptotics. Nonetheless, in a previous study on the NaCl molecule [59], an exponential distance dependence of $\kappa_{\mathrm{Na^+Cl^-}}$ allowed us to reproduce partial charges deduced from DFT-based calculations quite reasonably.

In a solid, the bond hardness terms can potentially have a more complex environment dependence than in molecules. As a starting point, we nevertheless assume their asymptotic, exponential form for the lack of an obvious, similarly simple alternative. In our parameterization study, we only consider such an environment dependence for an expansion around the ionic state and abbreviate the ensuing full method "environment-dependent redox

split-charge equilibration" as EDR-SQE. However, as a default, that is in all other CPTs studied here, we keep treating all hardness terms as constant.

One could certainly also expect $\kappa_{\mathrm{NaCl}}$ to be distant or environment dependent if one took neutral atoms as reference. However, this will not be investigated in this work for the following reason: Atomic reference states are only meaningful for bond lengths exceeding $\approx 3.7$ nm, at which point the difference between the ionization energy of sodium and the electron affinity of chlorine, $I_{\mathrm{Na}} - A_{\mathrm{Cl}} \approx 1.5$ eV exceeds the Coulomb interaction in the rocksalt structure.

Another environment-dependent term in a R-SQE model could be the electron affinity of an anion, e.g., $A_{\mathrm{Cl}^-}$. For an isolated anion, it should be very small, because the second excess electron will delocalize at a large distance of the original anion thereby keeping its kinetic energy as well as Coulomb and exchange interaction to a minimum. In a solid, however, the additional excess electron is effectively confined to the space attributed to the anion. This space becomes rather small at large pressure so that $A^-_{\mathrm{Cl}}$ can become a large negative number. As we have no model to account for this effect, we exclude large positive pressures from our EDR-SQE analysis.

It might be worth mentioning that including environment-dependent terms in an R-SQE model, such as distance dependent bond hardnesses, requires one to compute additional derivatives when calculating forces on atoms. In general, the evaluation of these derivatives can be implemented such that only few extra floating-point operations need to be conducted.

### D. Cauchy violation in CTPs at finite pressure

To discuss the effect of charge-transfer potentials on the Cauchy violation, we need to calculate the second-order derivatives of the energy $U_{\mathrm{CTP}}$ with respect to strain-tensor elements. We do this for the rocksalt structure but note that the equations are similar for other ionic solids with inversion symmetry.

Expanding the $U_{\mathrm{CTP}}\{\Delta\chi, \kappa_{\mathrm{C}}, Q\}$ in equation (40) around a (cubic) reference state, one time assuming a fixed charge of $Q = -\Delta\chi^2/\kappa_{\mathrm{C}}(\eta_{\mathrm{ref}})$ in the FC approach, and another time allowing charge transfer in the CTP approach, leads to the following relation for second derivatives of the energies

$$\begin{aligned}\frac{\partial^2 U(\mathrm{FC})}{\partial\eta_i\partial\eta_j} - \frac{\partial^2 U(\mathrm{CTP})}{\partial\eta_i\partial\eta_j} &= \frac{\Delta\chi^2}{\kappa_{\mathrm{C}}}\frac{\partial \ln\kappa_{\mathrm{C}}}{\partial\eta_i}\frac{\partial \ln\kappa_{\mathrm{C}}}{\partial\eta_j} \\ &= \kappa_{\mathrm{C}}\frac{\partial Q}{\partial\eta_i}\frac{\partial Q}{\partial\eta_j} \end{aligned} \tag{49}$$

This equation reveals that the Cauchy pressure contribution from charge transfer potentials in NaCl structures is strictly non-positive in cubic structures, since $\partial Q/\partial\eta_1 = \partial Q/\partial\eta_2$ is not identical zero unlike $\partial Q/\partial\eta_4$.

Including the possibility for a strain-dependence of the bond hardness, $\kappa_{\mathrm{NaCl}}(\eta)$, the following Cauchy pressure can be obtained from evaluating equation (49) around a cubic reference structure

$$\begin{aligned}-P_{\mathrm{C}} = \frac{1}{V_0}\Bigg\{\kappa_{\mathrm{C}}\left(\frac{\partial Q}{\partial\eta_1}\right)^2 \\ + \frac{Q^2}{24}\left(\frac{\partial^2\kappa_{\mathrm{NaCl}}}{\partial\eta_6^2} - \frac{\partial^2\kappa_{\mathrm{NaCl}}}{\partial\eta_1\partial\eta_2}\right)\Bigg\}.\end{aligned} \tag{50}$$

The second summand in the curly brackets on the r.h.s. of equation (50) can, in principle, take any aribitrary value. However, it disappears as long as the individual $\kappa_{\mathrm{NaCl}}$ are constant or merely distance dependent. In this approximation, CTP-induced Cauchy pressures are strictly negative and thus we still find that

$$C_{12}(\mathrm{CTP}) < C_{66}(\mathrm{CTP}). \tag{51}$$

### E. Born effective charges in CTPs

For a system without periodic boundary conditions, the dipole of a CTP system, assuming no on-site polarizability, is defined as

$$\mathbf{p} = \sum_j Q_j \mathbf{r}_j. \tag{52}$$

The Born effective charge tensor elements of atom $i$ then read

$$Q^*_{i,\alpha\beta} = Q_i\delta_{\alpha\beta} + \sum_j \frac{\partial Q_j}{\partial r_{i,\beta}} r_{j,\alpha}, \tag{53}$$

where we have expanded around neutral atomic references $n_j = 0\ \forall\ j$.

For periodically repeated systems, the dipole cannot be defined for reasons discussed in more detail in the literature [63]. However, an excess dipole $\Delta\mathbf{p}$ can be defined in a straightforward fashion in the context of models where charge transfer only occurs locally, as is the case in the AACT or the SQE model. One can then write

$$\Delta\mathbf{p} = \sum_{ij} q_{ij}\mathbf{r}_{ij}, \tag{54}$$

where the $\mathbf{r}_{ij}$ must abide the minimum-image conventions. The Born-charge tensor elements then become

$$Q^*_{i,\alpha\beta} = \sum_j \left(q_{ij}\delta_{\alpha\beta} + \frac{\partial q_{ij}}{\partial r_{ij,\beta}} r_{ij,\alpha}\right). \tag{55}$$

for a reference state consisting of neutral atoms. Thus, in general, the Born charge tensor of an atom is not simply proportional to the identity matrix. Instead, its symmetry reflects the symmetry of the environment into which the given atom is embedded.

When free ions are the reference, their integer charges

need to be added to the Born effective charge tensor in (55), i.e.,

$$Q^*_{i,\alpha\beta} \to n_i e\delta_{\alpha\beta} + Q^*_{i,\alpha\beta}. \tag{56}$$

The Born effective charge tensor is identical to the partial charge times the identity matrix as long as atoms is located in a site with inversion symmetry and induced dipoles are neglected. This is because the sum over the second term on the r.h.s. of equation (55) adds up to zero under these circumstances. Otherwise Born and partial charge may differ.

Since the $q_{ij}$ and the $\mathbf{r}_{ij}$ change sign upon reversing the order of their indices, the SQE-based Born effective charge tensors obey the so-called acoustic sum rule [64]

$$\sum_i Q^*_{i,\alpha\beta} = \sum_i n_i e\delta_{\alpha\beta}, \tag{57}$$

where the sum over all oxidation numbers on the r.h.s. of the equation is the net charge of the system.

## IV. RESULTS

### A. DFT results and force-field parameterization of fixed-charge potentials and conventional CTPs

In order to parametrize a potential, it is beneficial to have reliable, self-consistent, and sufficient data. Often, there is not enough experimental information to fully define the adjustable parameters in a meaningful fashion and/or to have a consistent set of data to test force-field based predictions. This is why we parametrize the force fields in the work exclusively to DFT-based data.

Our fixed-charge potential, which we consider for comparison purposes, has five adjustable parameters, $U_{0,\mathrm{NaCl}}$, $a_{\mathrm{NaCl}}$, $U_{0,\mathrm{CaCl}}$, $a_{\mathrm{ClCl}}$, and $Q_{\mathrm{Na}}$. In the conventional charge-transfer potential, $Q_{\mathrm{Na}}$ is no longer a parameter, but instead we need to adjust $\kappa_{\mathrm{T}}$ and $\Delta\chi$. Thus, we need to calibrate our potential against at least six independent reference data points. The parameterization of our EDR-SQE potential is handled differently than for the CTPs in which the (bond) hardness terms are treated constant, see section IV B.

As input reference data we chose: the lattice constant $a_0$, three independent components of the elastic tensor (rewritten as bulk modulus, Cauchy pressure, and anisotropy pressure), the two optical vibrational frequencies at the Γ-point $\omega_{\mathrm{LO,TO}}$ — all at mechanical equilibrium — as well as the pressure at one density 15% above and another density 15% below the equilibrium density (which allows one to fix the change of bulk modulus with pressure $B' = dB/dP$). The numbers are listed in table I.

To calibrate the parameters, we construct a $\chi^2$ penalty function according to

| | $a_0$ | $B_0$ | $-P_{\mathrm{C}}$ | $P_{\mathrm{A}}$ | $\omega_i$ | $P(V_i)$ |
|---|---|---|---|---|---|---|
| $w_n$ | 1 | 0.5 | 0.25 | 0.25 | 0.5 | 0.25 |
| $\Delta O_n$ | $0.01\,a_0$ | $0.1\,B_0$ | $0.1\,B_0$ | $0.1\,B_0$ | $0.05\,\omega_i$ | $0.1\,P(V_i)$ |

TABLE II. Significance and the weight of observables entering the fit.

$$\chi^2 = \frac{1}{\sum_n w_n}\sum_n w_n \frac{\{O_n - O_n(\mathrm{DFT})\}^2}{(\Delta O_n)^2}. \tag{58}$$

Here $O_n$ is the $n$'th observable as predicted by a model potential, $O_n$(DFT) the corresponding value from DFT, $\Delta O_n$ is the target accuracy of the observable, and $w_n$ is the weight of the observable reflecting its importance that we assign to it. The $\chi^2$ penalty function is therefore designed such that $\chi^2 = 1$ separates the domain where the target accuracies are reproduced on average from that where they are not achieved. The respective accuracies and weights are summarized in table II. The fits turn out rather robust, which means that as long as we do not alter the weights by an order magnitude, the deduced force field parameters vary only mildly.

The parameters obtained from minimizing our $\chi^2$ penalty function are listed in table III. The results for each parameterization are summarized in table IV.

We first discuss the results from our fits in the context of an expansion about neutral atoms. Taking values for electron affinities and ionization energies of neutral atoms, which were obtained from DFT, i.e., $A_{\mathrm{Cl}} \approx 5.5$ eV, $A_{\mathrm{Na}} \approx 2.1$ eV, $I_{\mathrm{Cl}} \approx 11$ eV, $I_{\mathrm{Na}} \approx 3.5$ eV, we would have expected $\Delta\chi \approx -2.7$ eV and $\kappa_{\mathrm{T}} = 3.5\ \mathrm{eV} + \kappa_{\mathrm{NaCl}}/12$. Thus, our result for $\Delta\chi$ is off by a factor of five. Moreover, the estimate for $\kappa_{\mathrm{NaCl}}$ would be 260 eV. This value seems unreasonably large, as one might expect $\kappa_{\mathrm{NaCl}}$ to correlate with the band gap of NaCl [15]. Given that the experimental band gap of rock salt is around 9 eV [66], the bond hardness turns out roughly thirty times greater than expected.

In the context of R-SQE, one also can assume most terms from DFT calculations, $A_{\mathrm{Na^+}} = I_{\mathrm{Na}}$, $I_{\mathrm{Na^+}} \approx 42$ eV, and $I_{\mathrm{Cl^-}} = A_{\mathrm{Cl}}$, however, $A_{\mathrm{Cl^-}}$ is not known and therefore treated as a fit parameter. Likewise, $\kappa_{\mathrm{Na^+Cl^-}}$ is deduced from the fit, i.e., $(\Delta\chi^\dagger, \kappa_{\mathrm{R}})$ in table III can be used to get estimates for $A_{\mathrm{Cl^-}}$ and $\kappa_{\mathrm{Na^+Cl^-}}$. Using the definitions from section III B one can write

$$A_{\mathrm{Cl^-}} = I_{\mathrm{Na^+}} + A_{\mathrm{Na^+}} - I_{\mathrm{Cl^-}} - 4\Delta\chi_{\mathrm{R}}. \tag{59}$$

We find a value of $A_{\mathrm{Cl^-}} = -3.05$ eV, which is perfectly meaningful, since it is energetically unfavorable to place an extra electron onto a chlorine ion. Solving a linear equation for $\kappa_{\mathrm{Na^+Cl^-}}$ in the R-SQE formalism leads to $\kappa_{\mathrm{Na^+Cl^-}} = 18.5$ eV. This value is only a factor of 2 higher than the experimental value rather than a factor of 30 as

| | $U_{0,\mathrm{NaCl}}$ | $a_{\mathrm{NaCl}}$ | $U_{0,\mathrm{ClCl}}$ | $a_{\mathrm{ClCl}}$ | $Q_{\mathrm{Na}}$ | $-\Delta\chi^{\dagger}$ | $\kappa_{\mathrm{T,R}}$ |
|---|---|---|---|---|---|---|---|
| Fixed point charges | 15362.0 | 0.2296 | 25.9 | 0.5973 | 0.88 | | |
| Fixed distributed charges | 36053.5 | 0.2082 | 51.7 | 0.5542 | 0.89 | | |
| CTP point charges | 48497.1 | 0.2067 | 59.5 | 0.5470 | | 14.32 | 25.11 |
| CTP distributed charges | 84291.8 | 0.1941 | 99.0 | 0.5124 | | 13.07 | 23.37 |

TABLE III. Force field parameters. The units are eV for energy, Å for length, and the elementary charge for charges. To describe distributed charges, Gaussians centered on atoms, atomic radii proposed by Shannon [65] were used: $R_{\mathrm{Na}} = 0.51$ Åand $R_{\mathrm{Cl}} = 0.91$ Å. The term $\Delta\chi^{\dagger}$ is identical to $\Delta\chi$ for an expansion about a reference of neutral atoms. In expansions about ions, $\Delta\chi^{\dagger}$ corresponds to $\Delta\chi_{\mathrm{R}} - \kappa_{\mathrm{R}}$.

| | $a_0$ | $B_0$ | $-P_{\mathrm{C}}$ | $P_{\mathrm{A}}$ | $\omega_{\mathrm{LO}}$ | $\omega_{\mathrm{TO}}$ | $P(V_{1,2})$ | $\chi^2$ |
|---|---|---|---|---|---|---|---|---|
| Fixed point charges | 5.607 | 25.8 | 0.00 | -5.83 | 248.0 | 135.2 | 7.24, -3.21 | 0.804 |
| Fixed distributed charges | 5.606 | 25.7 | 0.00 | -5.83 | 249.1 | 135.2 | 7.24, -3.19 | 0.794 |
| CTP point charges | 5.600 | 25.1 | 3.20 | -5.27 | 251.8 | 139.9 | 7.20, -2.93 | 0.511 |
| CTP distributed charges | 5.600 | 25.1 | 3.04 | -5.34 | 253.0 | 139.2 | 7.22, -2.90 | 0.573 |

TABLE IV. Learning set produced by models. The units are Å for length, GPa for pressure, and $\mathrm{cm}^{-1}$ for frequencies.

before. Thus, the adjustable parameters take physically meaningful values.

### B. Parametrization of EDR-SQE

An immediate consequence of treating (bond) hardness terms constant is that the partial charge of ions in rock salt (and other ionic solids) is generally predicted to increase monotonically with increasing pressure. The reason is that the Coulomb interactions favors large charges at small interatomic distances. However, in experimental [67] and DFT-based [68] studies of ionic crystals – and also in our DFT calculations of rock salt – the trend is opposite: partial charges (Bader or effective Born, different in DFT but identical in CTPs that do not consider dipoles on atoms) initially increase when bond lengths are stretched from equilibrium to larger distances, even if the ultimate dissociation limit should be neutral atoms. These trends are revealed for NaCl in figure 1, where we show not only Born effective charges but also Bader charges.

To reproduce the correct trend, we follow the suggestion [59] to expand SQE around ions and to make the combined hardness increase when the bonds are stretched. We name such an expansion environment-dependent redox (EDR) split-charge equilibration (SQE), or EDR-SQE. For the NaCl dimer, a reasonable description of partial charges was given by introducing an exponential distance dependence of the bond hardness [59]. Unfortunately, there can be a more general environment dependence of the (bond) hardness terms in the bulk. The simplest approach giving reasonable (Bader) charges

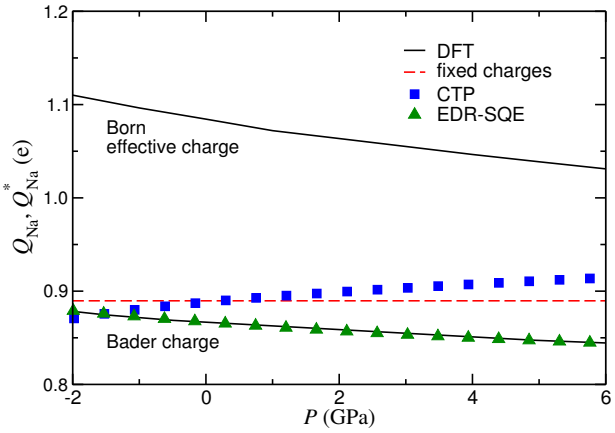


FIG. 1. Born effective and Bader charges (different in DFT but identical in the other shown approaches) as a function of the isotropic pressure $P$ as obtained by DFT, by the fixed charges approximation, the conventional charge-transfer potential (CTP), and the environment-dependent redox-split-charge equilibration (EDR-SQE) potential.

is to make the total hardness an exponential function of the bond length $a$. Assuming $A_{\mathrm{Cl}^-} = -12.1$ eV and $\kappa_{\mathrm{T}}(a) = 2.66\,\mathrm{eV}\,\exp(-a/0.928\,\text{Å})$ while keeping all other ionic terms fixed to their experimental values gives the EDR-SQE charge shown in figure 1. The short-range interactions of the EDR-SQE were then fitted to the same set of data as the other CTPs. We only excluded the Cauchy and the anisotropy pressure from the parameterization, as their fit would have necessitated knowledge of the environment dependence of the total hardness beyond

| | $U_{0,\mathrm{NaCl}}$ | $a_{\mathrm{NaCl}}$ | $U_{0,\mathrm{ClCl}}$ | $a_{\mathrm{ClCl}}$ |
|---|---|---|---|---|
| EDR-SQE point-charges | 438.4 | 0.3683 | 0.01046 | 2.664 |

TABLE V. Short-range interaction parameters of the redox-SQE force field with environment-dependent bond hardness term. The units are eV for energy, Å for length.

isotropic compression. The adjustable parameters defining the short-range interaction in EDR-SQE are listed in table V

### C. Pressure dependence of selected quantities

To investigate the quality of potentials outside the domain of the learning set, we compute the pressure dependence of most quantities on which the adjustable parameters were gauged. However, we restrict our attention to three cases, which are representative for a number of possibilities that result from switching "on" or "off" the following options: short-range repulsion between chlorine anions, distributed charges, charge transfer. In the latter case we can furthermore ignore or consider an ionic reference state and an environment dependent chemical hardness. Out of these possibilities, we decided to consider one fixed-charge, one conventional charge-transfer potential, one charge transfer potential with non-zero reference redox state and EDR-SQE. In all four cases, we include the short-range repulsion between chlorine atoms, as it is not possible otherwise — in the realm of the potential surfaces investigated here — to obtain reasonably accurate optical frequencies in the Γ point. For the fixed-charge approach we used distributed charges, while for the fluctuating charge models we used point charges, as these gave slightly better fits near equilibrium for the respective treatments for the system in either case. We note that this means only one additional adjustable parameter for the charge-transfer potential, as many of its parameters are taken either from DFT or from the literature and not fine tuned any further. This includes the screening lengths for short-range Coulomb interactions as well as the ionization energies and electron affinities of the involved atoms or ions. Thus, in one case, we have the fixed charge as a fit parameter, and in the other case a total hardness as well as an effective electronegativity.

We start the analysis of our "test set" with the pressure dependence of the Cauchy pressure in Fig. 2. One can readily notice that the charge-transfer potentials produce the Cauchy pressure with the correct sign at ambient conditions. However, they overcorrect it by a non-negligible amount compared to a fixed-charge approach, for which $P_{\mathrm{C}}$ in rock salt disappears by definition. Yet, the charge-transfer potentials produce the correct trend, that is, the negative of the Cauchy violation increases with increasing isotropic pressure $P$.

We note that it appears necessary to induce another many-body term into our force field in addition to charge

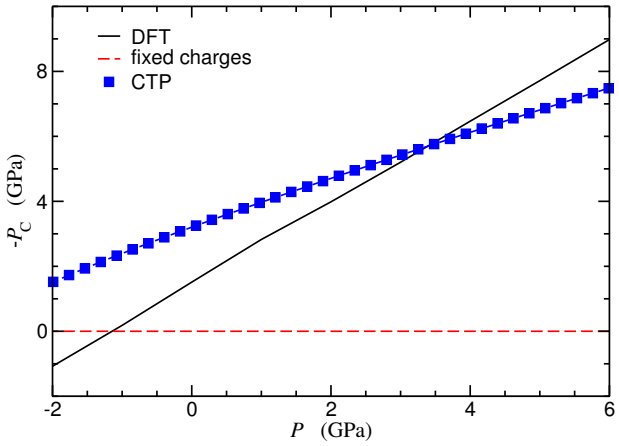


FIG. 2. Negative of the Cauchy pressure $P_{\mathrm{C}}$ as a function of the isotropic pressure $P$ obtained either by DFT or the fixed-distributed-charges approximation, or the point-charge-transfer potential, or environment-dependent redox-SQE point charges potential. Dashed lines represent the analytical solutions according to equation (50).

transfer, i.e., one that counteracts the overestimation of $-P_{\mathrm{C}}$ and that can reproduce positive Cauchy pressures for $P < -2$ GPa. A natural candidate for this would be to augment the charge-transfer potential with terms deriving from quasi-atom theory, as done, for example, by Streitz and Mintmire [69]. Such additional terms naturally lead to positive Cauchy pressures. We abstain from parametrizing such a potential here, as the focus of this study is on investigating the generic effects of charge-transfer potentials on physical properties rather than on designing a highly accurate and transferable potential. To achieve the latter, our aim would be — as in our design of potential for copper [70] — to construct it such that the potential does not only work for a single geometry, i.e., for rock salt but for many different bonding environments. Such an endeavor is outside of the present scope.

We next investigate the equation of state (EOS) in figure 3. The fixed-charge approach appears to reproduce the EOS slightly better than conventional CTPs, however, differences are only minor. In these two cases, the predicted isotropic pressure becomes too large at large densities, which could mean that the exponential repulsion is too stiff at high compression. However, the EDR-SQE model, which best reproduces the EOS, underestimates the pressure at small volumes. We conclude that the EOS is an unsuitable function on which to gauge adjustable, charge-transfer related parameters.

The pressure dependence of longitudinal and transverse optical frequencies in the Γ point also turns out rather insensitive to whether charges are fixed or adjustable, as one can see in figure 4. This result, however, can be readily rationalized: for crystals in which each atom has an equilibrium position with inversion symmetry, induced charges can only be quadratic in the dis-

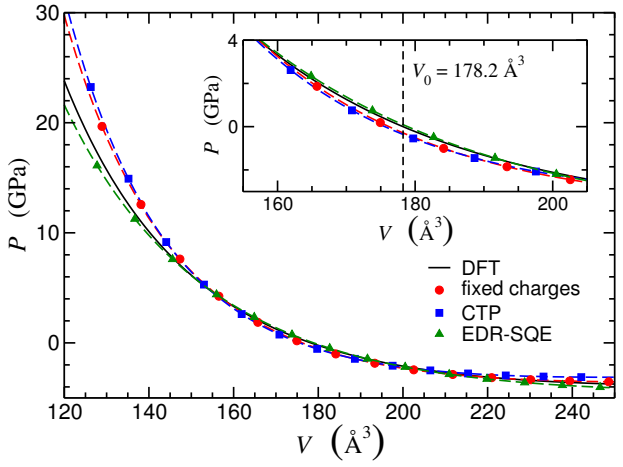


FIG. 3. Equation of state, $P(V)$, as obtained by DFT, by the fixed-distributed-charge approximation, the point-charge-transfer potential, and the environment-dependent redox-SQE point charges potential. The inset shows the equation of state with larger magnification around small pressures.

placement of an optical Γ-point vibration. As such, Γ-point frequencies remain unaffected by the charge transfer induced by an optical Γ-point vibration. This time, the EDR-SQE model appears to show the least satisfactory agreement with the DFT data. This shortcoming might have been expected as we have not optimized the general strain dependence of the total hardness beyond isotropic compression. However, as we demonstrate next, EDR-SQE best reproduces how the LO-TO splitting depends on pressure.

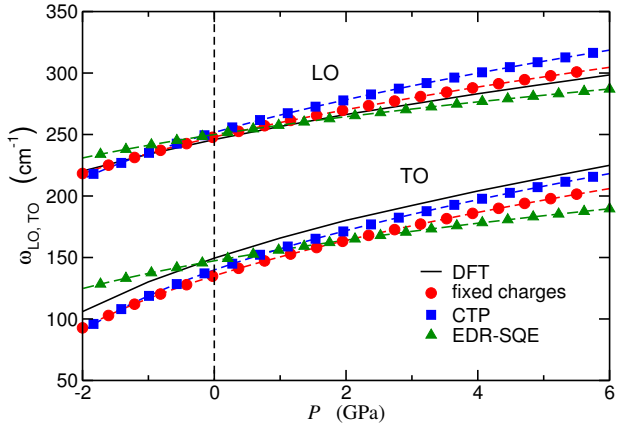


FIG. 4. Longitudinal ($\omega_{\rm LO}$) and transverse ($\omega_{\rm TO}$) optical Γ-point frequencies as a function of the isotropic pressure $P$ as obtained by DFT, by the fixed-distributed-charges approximation, the point-charge-transfer potential, and the environment-dependent redox-SQE point charges potential.

In figure 5 we show the pressure dependence of the LO-TO splitting as a function of pressure $P$. More specifically, we show the splitting $\omega_{\rm LO}^2 - \omega_{\rm TO}^2$ times the volume of the primitive unit cell, $V_{\rm p}$, as this product is constant in a fixed-charge approach. Conventional CTPs without environment-dependent or bond-length-dependent chemical hardnesses predict the wrong slope for how our measure for the LO-TO splitting depends on pressure. This was to be expected, as the LO-TO splitting is induced by the long-range electric fields of the (Born effective) charges [36]. In fact, the ratio $V_{\rm p}(\omega_{\rm LO}^2 - \omega_{\rm TO}^2)/(Q^*_{\alpha\alpha})^2$ turns out to be insensitive to density. Thus, since the conventional CTPs predict the wrong sign of $\mathrm{d}Q/\mathrm{d}P$, they also predict the wrong trend for how our measure for the LO-TO splitting depends on $P$.

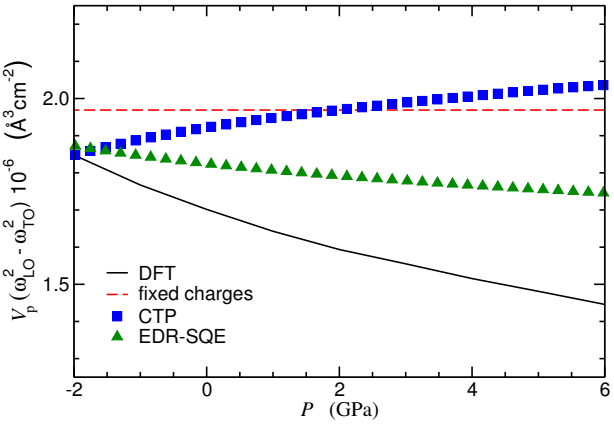


FIG. 5. Measure for the LO-TO splitting, $V_{\rm p}\left(\omega_{\rm LO}^2 - \omega_{\rm TO}^2\right)$, as a function of the isotropic pressure $P$ as obtained by DFT, by the fixed-distributed-charges approximation, the point-charge-transfer potential, and the environment-dependent redox-SQE point charges potential. $V_{\rm p}$ is the primitive cell volume.

The EDR-SQE potential predicts the correct trend for how our measure for the LO-TO splitting depends on $P$; however, the slope turns out too small. This shortcoming could have also been expected since the Bader charges, on which we parametrized the potential, show a smaller pressure dependence than the Born effective charges. We deduce from figure 5 that charge transfer only accounts for roughly 25% of the pressure dependence of the LO-TO splitting. The missing contribution must come from the atomic polarizability, which can be reflected, for example, by models originally proposed by Madden and Wilson [10, 71].

## V. CONCLUSIONS

The first main result of this study is that charge transfer potentials generally induce a negative contribution to the Cauchy pressure, which increases in magnitude with increasing density. This type of behavior is revealed in rock salt, however, to a lesser extent than one would expect if charge transfer were the only many-body interaction. Thus, it seems as if additional many-body ef-

fects inducing positive Cauchy pressures were needed for this — and in all likelihood for any — ionic solid. An ionic solid for which charge transfer might dominate the Cauchy pressure even at ambient pressure is lithium hydride (LiH). Like NaCl, LiH has no directed bonds and crystallizes in the rocksalt lattice. However, the value for $C_{44} \approx 48$ GPa exceeds that for $C_{12} \approx 14$ GPa by more than a factor of three, which results in a Cauchy pressure of $-34$ GPa [72].

Our analysis also reveals that, as long as the environment dependence of bond hardnesses is ignored, different charge-transfer approaches are formally equivalent as far as structural or elastic Γ-point properties are concerned, e.g., elastic tensor, equation of state, Γ-point optical phonons and even partial or Born effective charges. Results can also be identical between CTPs expanding around the atomic or the ionic reference state. In this sense, fitting adjustable parameters to Γ-point properties does not allow one to ascertain which CTP is the best suited. This might be counterintuitive as the dielectric response function of different CTPs can differ quite substantially, i.e., conventional CTPs treats systems as perfect metals, while the split-charge model behaves like a dielectric unless the bond hardness is set to zero, in which case SQE reduces to a conventional CTP.

The difference between various CTP approaches without environment-dependent hardnesses (in regard to Γ point properties) lies in the numerical values for the parameters and their subsequent interpretation. For example, if we parametrized our potential relative to neutral atoms and used reasonable values for electron affinities and ionization energies, then we would need to boost the hardness term by as much as 22 eV. Irrespective of whether the boost of hardnesses is placed directly as an environment correction to the atomic hardnesses (the measured combined hardness being 3.5 eV) or as an extra bond hardness (which would need to be as large as 260 eV), the added hardness would have to be called meaningless. The increase of the electronegativity difference between Na and Cl atoms from 5 eV for free atoms to 29 eV in the crystal appears to be even more nonsensical. In contrast, when the parameterization is interpreted as being an SQE expansion around ionic states, we only need to introduce a bond hardness of 18 eV. This is perfectly meaningful, as the SQE bond hardness can be interpreted as a measure for the band gap, which in NaCl happens to be 9 eV.

Models with constant bond hardness predict a decrease in the Born effective charges, as well as formal atomic charges, with increasing bond length, which is contrary to DFT results. In order to fix this issue one can introduce environment-dependent (bond) hardnesses, which should increase monotonically at large separations. In the simplest approach, one could assume that the (bond) hardness is simply an exponential function of the bond length. While this approach allows one to reproduce (Bader) charges reasonable well, reality might be more complicated. A simple bond-length dependence of the (bond) hardness leads to a rather large overestimation of the (negative) Cauchy pressure. The correct functional dependencies for the (hardness) parameters in charge transfer potentials remains to be researched.

## ACKNOWLEDGMENTS

The authors thank the Jülich Supercomputing Centre for computing time on JUROPA and Jari Jalkanen for useful discussions.

[1] M. Born and K. Huang, *Dynamical Theory of Crystal Lattices* (Oxford: Clarendon Press, 1954).
[2] E. G. Brovman, Y. Kagan, and A. Kholas, J. Exp. Theor. Phys. **30**, 883 (1970).
[3] M. W. Finnis and J. E. Sinclair, Philos. Mag. A **50**, 45 (1984).
[4] M. S. Daw and M. I. Baskes, Phys. Rev. B **29**, 6443 (1984).
[5] G. D. Mahan, Phys. Rev. B **29**, 5849 (1984).
[6] Y. Liang, C. R. Miranda, and S. Scandolo, J. Chem. Phys. **125**, 194524 (2006).
[7] B. G. Dick and A. W. Overhauser, Phys. Rev. **112**, 90 (1958).
[8] J. O. Hirshfelder, C. F. Curtiss, and R. B. Bird, *Molecular Theory of Gases and Liquids* (Wiley, New York, 1954).
[9] W. L. Bade and J. G. Kirkwood, J. Chem. Phys. **27**, 1284 (1957).
[10] M. Salanne, B. Rotenberg, S. Jahn, R. Vuilleumier, C. Simon, and P. A. Madden, Theor. Chem. Acc. **131**, 1143 (2012).
[11] U. Shröder, Solid State Commun. **4**, 347 (1966).
[12] C. Sanjeeviraja, K. Kesavasamy, N. Krishnamurthy, and S. K. Mohanlal, J Phys Chem Solids **45**, 651 (1984).
[13] M. Matsui, J. Chem. Phys. **108**, 3304 (1998).
[14] M. Matsui, S. C. Parker, and M. Leslie, Am. Mineral. **85**, 312 (2000).
[15] M. H. Müser, Eur. Phys. J. B **85**, 135 (2012).
[16] W. J. Mortier, S. K. Ghosh, and S. Shankar, J. Am. Chem. Soc. **108**, 4315 (1986).
[17] D. M. York and W. Yang, J. Chem. Phys. **104**, 159 (1996).
[18] R. Chelli, P. Procacci, R. Righini, and S. Califano, J. Chem. Phys. **111**, 8569 (1999).
[19] R. A. Nistor, J. G. Polihronov, M. H. Müser, and N. J. Mosey, J. Chem. Phys. **125**, 094108 (2006).
[20] T. Verstraelen, P. W. Ayers, V. V. Speybroeck, and M. Waroquier, J. Chem. Phys. **138**, 074108 (2013).
[21] R. T. Sanderson, Science **114**, 670 (1951).
[22] L. D. Landau and E. M. Lifshitz, *Theory of Elasticity* (Pergamon, London, 1959).
[23] F. D. Murnaghan, *Finite Deformation of an Elastic Solid*

(John Wiley & Sons, Inc., New York, 1951).
[24] R. N. Thurston, J. Acoust. Soc. Am. **37**, 348 (1965).
[25] J. H. Weiner, *Statistical Mechanics of Elasticity* (John Wiley & Sons, New York, 1983).
[26] F. Birch, Phys. Rev. **71**, 809 (1947).
[27] K. Brugger, Phys. Rev. **133**, A1611 (1964).
[28] D. C. Wallace, Phys. Rev. **162**, 776 (1967).
[29] F. Milstein and R. Hill, J. Mech. Phys. Solids **27**, 255 (1979).
[30] J. Wang, S. Yip, S. R. Phillpot, and D. Wolf, Phys. Rev. Lett. **71**, 4182 (1993).
[31] R. S. Mulliken, J. Chem. Phys **23**, 1833 (1955).
[32] R. F. W. Bader, *Atoms in Molecules: A Quantum Theory* (Clarendon, Oxford, 1990).
[33] F. L. Hirshfeld, Theor. Chim. Acta **44**, 129 (1977).
[34] J. F. Gonthier, S. N. Steinmann, M. D. Wodrich, and C. Corminboeuf, Chem. Soc. Rev. **41**, 4671 (2012).
[35] T. Verstraelen, P. W. Ayers, V. V. Speybroeck, and M. Waroquier, J. Chem. Theory Comput. **9**, 2221 (2013).
[36] R. H. Lyddane, R. G. Sachs, and E. Teller, Phys. Rev. **59**, 673 (1941).
[37] R. Resta, M. Posternak, and A. Baldereschi, Phys. Rev. Lett. **70**, 1010 (1993).
[38] R. Resta, Rev. Mod. Phys. **66**, 899 (1994).
[39] G. Henkelman, A. Arnaldsson, and H. Jónsson, Comput. Mater. Sci. **36**, 354 (2006).
[40] E. Sanville, S. D. Kenny, R. Smith, and G. Henkelman, J. Comp. Chem. **28**, 899 (2007).
[41] W. Tang, E. Sanville, and G. Henkelman, J. Phys.: Condens. Matter **21**, 084204 (2009).
[42] P. Hohenberg and W. Kohn, Phys. Rev. **136**, B864 (1964).
[43] W. Kohn and L. J. Sham, Phys. Rev. **140**, A1133 (1965).
[44] P. Giannozzi, S. Baroni, N. Bonini, M. Calandra, R. Car, C. Cavazzoni, D. Ceresoli, G. L. Chiarotti, M. Cococcioni, I. Dabo, A. D. Corso, S. de Gironcoli, S. Fabris, G. Fratesi, R. Gebauer, U. Gerstmann, C. Gougoussis, A. Kokalj, M. Lazzeri, L. Martin-Samos, N. Marzari, F. Mauri, R. Mazzarello, S. Paolini, A. Pasquarello, L. Paulatto, C. Sbraccia, S. Scandolo, G. Sclauzero, A. P. Seitsonen, A. Smogunov, P. Umari, and R. M. Wentzcovitch, J. Phys.: Condens. Matter **21**, 395502 (2009).
[45] J. P. Perdew, K. Burke, and M. Ernzerhof, Phys. Rev. Lett. **77**, 3865 (1996).
[46] A. D. Becke, Phys. Rev. A **38**, 3098 (1988).
[47] J. P. Perdew, J. A. Chevary, S. H. Vosko, K. A. Jackson, M. R. Pederson, D. J. Singh, and C. Fiolhais, Phys. Rev. B **46**, 6671 (1992).
[48] N. Troullier and J. L. Martins, Phys. Rev. B **43**, 1993 (1991).
[49] C. Hartwigsen, S. Goedecker, and J. Hutter, Phys. Rev. B **58**, 3641 (1998).
[50] P. E. Blöchl, Phys. Rev. B **50**, 17953 (1994).
[51] H. J. Monkhorst and J. D. Pack, Phys. Rev. B **13**, 5188 (1976).
[52] J. M. Brown, J. App. Phys. **86**, 5801 (1999).
[53] A. M. Hofmeister, Phys. Rev. B **56**, 5835 (1997).
[54] J. T. Lewis, A. Lehoczky, and C. V. Briscoe, Phys. Rev. **161**, 877 (1967).
[55] R. Q. Fugate and D. E. Schuele, J. Phys. Chem. Solids **27**, 493 (1966).
[56] H. J. C. Berendsen, J. R. Grigera, and T. P. Straatsma, J. Phys. Chem. **91**, 6269 (1987).
[57] M. P. Tosi, Solid State Phys. **16**, 1 (1964).
[58] J. Cioslowski and S. T. Mixon, J. Am. Chem. Soc. **115**, 1084 (1993).
[59] W. B. Dapp and M. H. Müser, Eur. Phys. J. B **86**, 337 (2013).
[60] W. B. Dapp and M. H. Müser, J. Chem. Phys. **139**, 064106 (2013).
[61] N. Onofrio and A. Strachan, J. Chem. Phys. **143**, 054109 (2015).
[62] T. Verstraelen, E. Pauwels, F. D. Proft, V. V. Speybroeck, P. Geerlings, and M. Waroquier, J. Chem. Theory Comput. **8**, 661 (2012).
[63] D. Herzbach and M. H. Müser, Comp. Phys. Commun. **174**, 17 (2006).
[64] L. J. Sham, Phys. Rev. **188**, 1431 (1969).
[65] R. D. Shannon, Acta Cryst. **A32**, 751 (1976).
[66] D. M. Roessler and W. C. Walker, Phys. Rev. **166**, 599 (1968).
[67] J. S. Reparaz, L. R. Muniz, M. R. Wagner, A. R. Goñi, M. I. Alonso, A. Hoffmann, and B. K. Meyer, Appl. Phys. Lett. **96**, 231906 (2010).
[68] A. R. Oganov, M. J. Gillan, and G. D. Price, J. Chem. Phys. **118**, 10174 (2003).
[69] F. H. Streitz and J. W. Mintmire, Phys. Rev. B **50**, 11996 (1994).
[70] J. Jalkanen and M. H. Müser, Modelling Simul. Mater. Sci. Eng. , in print (2015).
[71] M. Wilson and P. A. Madden, J. Phys.: Condens. Matter **5**, 2687 (1993).
[72] B. W. James and H. Kheyrandish, J. Phys. C: Solid State Phys. **15**, 6321 (1982).